

Argandite, $\text{Mn}_7(\text{VO}_4)_2(\text{OH})_8$, the V analogue of allactite from the metamorphosed Mn ores at Pipji, Turtmann Valley, Switzerland

JOËL BRUGGER,^{1,2,*} PETER ELLIOTT,^{1,2} NICOLAS MEISSER,³ AND STEFAN ANSERMET³

¹Tectonics, Resources and Exploration (TRaX), School of Earth and Environmental Sciences, The University of Adelaide, North Terrace, 5005 Adelaide, South Australia

²Division of Mineralogy, South Australian Museum, North Terrace, 5000 Adelaide, South Australia

³Musée Géologique Cantonal and Laboratoire des Rayons-X, Institut de Minéralogie et de Géochimie, UNIL-BFSH2, CH-1015 Lausanne-Dorigny, Switzerland

ABSTRACT

Argandite, $\text{Mn}_7(\text{VO}_4)_2(\text{OH})_8$, is a new mineral from the metamorphosed syndimentary exhalative Mn deposit located underneath the Pipji glacier (Pipjigletscher) in the Turtmann valley, Central Alps, Switzerland. The mineral is dedicated to the Swiss geologist Émile Argand (1879–1940). Argandite occurs in manganosite-rich ores in association with the V-minerals pyrobelonite, reppiaite, and an unknown silico-vanadate with chemical formula $(\text{Mn},\text{Mg})_{24}(\text{V},\text{As},\text{Si})_4\text{Si}_2\text{O}_{27}\text{H}_{38}$; these minerals result from the remobilization of ore components during the Tertiary Alpine metamorphism under upper greenschist facies conditions (~450 °C, 4–6 kbar). Argandite forms isolated anhedral grains up to 60 μm in diameter. The mineral is transparent, orange in color with a pale orange streak and vitreous luster, Mohs hardness ~3.5–4, D_{calc} 3.67(1), and D_{meas} 3.71(5) g/cm^3 . It is brittle with one distinct cleavage, probably parallel to $\{001\}$. Argandite is biaxial negative, with $\alpha \sim 1.74$, $\beta = 1.762(4)$, $\gamma \sim 1.77$ (white light), $2V(\text{calc}) = -62^\circ$. It shows a distinct pleochroism under polarized light, orange-yellow to orange. The empirical chemical formula is $(\text{Mn}_{6.54}\text{Mg}_{0.38}\text{Ni}_{0.04}\text{Ca}_{0.02}\text{Zn}_{0.01}\text{Sr}_{0.01})_{\Sigma=7.00}(\text{V}_{1.46}\text{As}_{0.54})_{\Sigma=2.00}\text{O}_8(\text{OH})_{8.00}$. Argandite is monoclinic, space group $P2_1/n$, $a = 5.5038(2)$, $b = 12.2665(5)$, $c = 10.1055(5)$ Å, $\beta = 95.559(4)^\circ$; $V = 679.04(5)$ Å³; $Z = 2$. The six strongest lines measured in the X-ray powder diffraction pattern are [d in Å (I)(hkl)]: 3.074 (100)(131), 2.687 (70)(140;113), 3.395 (60)(112), 3.708 (50)(11 $\bar{2}$;121), 2.945 (50)(041;11 $\bar{3}$), and 2.522 (50)(004;20 $\bar{2}$). The crystal structure was solved with direct methods on the basis of 1661 unique reflections with $I > 4\sigma_F$ and refined to $R_1 = 3.40\%$. Argandite is isostructural with allactite, $\text{Mn}_7(\text{AsO}_4)_2(\text{OH})_8$, and raadeite, $\text{Mn}_7(\text{PO}_4)_2(\text{OH})_8$.

Keywords: Argandite, new mineral, crystal structure, metamorphosed exhalative Fe-Mn deposit, Turtmann valley, Central Alps, Switzerland

INTRODUCTION

Metamorphosed Mn-rich deposits, such as the ones at Långban in Sweden, the Kombat mine in Namibia, and at Franklin, New Jersey, U.S.A., are among the richest mineralogical “rainforests” on Earth (Pring 1995) and are still contributing a steady stream of minerals new to science. Many of these minerals contain arsenic or vanadium as a major component. In this paper, we describe the occurrence and mineralogy of argandite, a new manganese vanadate from the Barrhorn Unit under the Pipji glacier in the Turtmann valley, Valais, Switzerland.

The new mineral is dedicated to the Swiss geologist Émile Argand (1879–1940) for his contribution to understanding Alpine geology in general, and the geology of Turmanntal in particular. Thrust sheet tectonics was first observed by Gerlach (1869), but Argand’s (1911) seminal paper, based on the geology of the Turtmann valley, played a critical role in establishing the concept. Argand was an early proponent of Alfred Wegener’s theory of continental drift, advocating that plate tectonics and continental collisions were the best explanation for the forma-

tion of the Alps. His pioneering work elucidated the relationship between the various geologic provinces of the Western Alps. His map and cross sections are remarkably similar to modern versions (Argand 1916).

The new mineral and its name have been approved by the International Mineralogical Association (proposal number 2010-021). The holotype specimen is deposited in the Geological Museum, Lausanne, Switzerland (registration number MGL90369). Part of this holotype specimen is deposited in the South Australian Museum, Adelaide, South Australia (registration number G32923).

THE MN-FE LENSES AT PIPJI

The Turtmann valley (Turtmanntal), a tributary to the Rhone Valley in Canton Wallis, Central Alps, Switzerland, is geologically located in the Middle Penninic (Briançonnais Domain) Siviez-Mischabel super-nappe (Escher et al. 1987). In the upper part of the valley, the pre-Mesozoic crystalline rocks of the “Ensemble de l’Ergischhorn” are overlain by the sediments of the Barrhorn Series, one of the rare Mesozoic covers of the Briançonnais domain that is still bound to its original basement (Sartori 1990). In the cliff underneath the Pipji glacier (coordinates on the Swiss

* E-mail: joel.brugger@adelaide.edu.au

National Reference System: 112.450/622.550; 3030 m), several flattened lenses measuring up to 1×0.3 m contain black Mn-Fe ores (Brugger and Meisser 2006; Sartori 1990). These lenses are embedded in gray dolomitic marbles of the Ladinian "Couches à C. Goldfussi". The Mn-Fe ores and their host rocks have been subjected to a Tertiary regional metamorphism culminating at a temperature of about 450 °C and a pressure between 4 and 6 kbar (upper greenschist facies conditions; Sartori 1990). Brugger and Meisser (2006) showed that the lenses represent metamorphosed, synsedimentary, submarine-exhalative deposits, and not paleokarst filling as originally thought (Sartori 1990). The pre-metamorphic mineral assemblage most likely consisted of highly oxidized (Fe^{3+} , Mn^{4+}) chemical sediments deposited from low-temperature (<60 °C) hydrothermal fluids upon mixing with seawater at or near the seafloor.

OCCURRENCE AND CONDITIONS OF FORMATION OF ARGANDITE

Argandite occurs sparingly in the Mn-Fe lenses at Pipji. The mineral was first identified by Brugger and Meisser (2006) on the basis of electron microprobe analyses, and referred to as Unknown no. 1. Argandite occurs as a rock-forming mineral in a manganosite-rich specimen. It forms orange anhedral grains up to 60 μm in diameter (see Fig. 4g in Brugger and Meisser 2006), and is associated with the vanadates pyrobelonite [(Pb,Sr,Ba)(Mn,Ca)(VO₄)(OH)], reppiaite $\{Mn_5[(V,As)O_4]_2(OH)_4\}$, and Unknown no. 2 [(Mn,Mg)₂₄(V,As,Si)₄Si₂O₂₇H₃₈] (Brugger and Meisser 2006). Other metamorphic minerals from the Mn-rich ores include: jacobsonite, manganosite, magnetite, galaxite, pyrophanite, crednerite, kutnohorite, calcite, dolomite, spessartine, tephroite, manganocummingtonite, pennantite, fluorapatite, turtmannite, sarkinite, barite, pyrite, chalcopyrite, bornite(?), native copper, and algodonite. Quaternary weathering resulted in the formation of birnessite, takanelite, nsutite-ramsdellite, hollandite, manganite, pyrolusite, cuprite, and malachite.

Arsenate and vanadate species are easily absorbed on oxyhydroxides of Fe and Mn (Bowell 1994; Sherman and Randall 2003), and consequently they are enriched in all types of Fe- and Mn-rich sediments (Brugger and Meisser 2006). Brugger and Gieré (2000) suggest that in exhalative seafloor deposits, high V contents are associated with a hydrogenous origin, whereas a high As:V ratio indicates a proximal hydrothermal input. The carbonate-hosted exhalative ores from Val Ferrera, Switzerland, are found in a similar geological environment as those from Pipji (similar timing, tectonic setting, and host rock). The As and V contents of the Val Ferrera Fe-Mn ores plot along two independent trends, one As-rich and one V-rich, while the Pipji ores all have V:As ratios $\geq \sim 1$ (Brugger and Meisser 2006). This difference in bulk ore chemistry appears to control the difference in As-V mineralogy between the two occurrences. Vanadates dominate at Pipji (Brugger et al. 2001; Brugger and Meisser 2006), but in Val Ferrera different ore lenses, or different locations within the major lenses, are either As rich or V rich (Brugger and Gieré 1999, 2000); accordingly they contain either As-rich (Brugger and Berlepsch 1997; Brugger et al. 1997, 1998) or V-rich minerals (Brugger and Berlepsch 1996; Brugger et al. 2003, 2006).

Hence, argandite formed as a result of upper greenschist

facies metamorphism of exhalative Mn-Fe ores enriched in V relative to As.

APPEARANCE, PHYSICAL AND OPTICAL PROPERTIES

Argandite occurs as isolated anhedral grains up to 60 μm in diameter within the rock matrix. Argandite is orange in color with a pale orange streak. It is transparent with a vitreous luster and does not fluoresce under the UV lamp. The Mohs hardness was estimated to be 3.5–4. Argandite is biaxial negative, and $2V$ (calc) is $\sim 62^\circ$. The refractive indices were measured at 24 °C by the immersion method in Cargille liquids (white light) to be $\alpha \sim 1.74(1)$, $\beta = 1.762(2)$, and $\gamma \sim 1.77(1)$; average ~ 1.76 . The average refractive index calculated using the Gladstone-Dale relationship is 1.857; this value was obtained using the constants of Mandarino (1976), the average chemical analysis of Table 1 normalized to a sum of 100%, and a density of 3.68 g/cm³. This corresponds to a poor compatibility index [$(1 - \kappa_p/\kappa_c) = 0.112$]; however, such poor agreement also has been found for some well-characterized vanadates such as vanadinite and descloizite (Mandarino 2007). Argandite displays a distinct orange-yellow to orange pleochroism. Argandite is slowly soluble in cold 10% HCl. The mineral is brittle and has one distinct cleavage. The direction of the cleavage could not be determined, but by analogy with allactite, this cleavage is expected to be parallel to {001}. The measured density of 3.71(5) g/cm³ was obtained by the immersion method using a mixture of water and thallium malonate/formate (Clerici liquor). The density calculated using the unit-cell volume from the single-crystal refinement (see below) is 3.676 g/cm³ for the empirical formula and 3.670 g/cm³ for the simplified ideal formula.

CHEMICAL COMPOSITION

Chemical analyses were carried out with a Cameca SX51 electron microprobe operated at 15 kV, 10 nA, with counting times of 10 s on the peaks and 5 s on each side of the peak for background. The beam was tightly focused, but scanned over a $5 \times 5 \mu m^2$ area during analysis to limit beam damage. The empirical chemical formula obtained for argandite, based upon normalization on 9 cations and 8 H atoms per formula unit is $(Mn_{6.54}Mg_{0.38}Ni_{0.04}Ca_{0.02}Zn_{0.01}Sr_{0.01})_{\Sigma=7.00}(V_{1.46}As_{0.54})_{\Sigma=2.00}O_8(OH)_{8.00}$ (Table 1), leading to the simplified chemical formula $Mn_7(VO_4)_2(OH)_8$. The largest variance was observed for As (Table 1), and a plot of As vs. V shows a negative correlation between As and V, suggesting that the variation in the As content is related to substitution for V (Fig. 1). Note that SiO₂ was monitored and found to be below

TABLE 1. Electron microprobe micro-chemical analysis of argandite

Constituent	wt%	Range	St. dev.	Probe standard
V ₂ O ₅	17.27	16.85–17.85	0.26	vanadium metal
As ₂ O ₅	8.16	7.03–8.77	0.44	gallium arsenide
CaO	0.16	0.12–0.22	0.03	hydroxylapatite
MgO	2.02	1.82–2.15	0.08	almandine
MnO	60.49	59.9–61.29	0.33	rhodonite
NiO	0.36	0–0.48	0.12	pentlandite
ZnO	0.10	0–0.39	0.11	sphalerite
SrO	0.09	0.02–0.16	0.03	celestite
H ₂ O _{calc} *	9.40			
Total	98.05			

Note: Average of 23 analyses.

* Calculated to charge balance, assuming a total of nine cations per formula unit. Empirical formula $(Mn_{6.54}Mg_{0.38}Ni_{0.04}Ca_{0.02}Zn_{0.01}Sr_{0.01})_{\Sigma=7.00}(V_{1.46}As_{0.54})_{\Sigma=2.00}O_8(OH)_{8.00}$.

the detection limit of 0.05 wt% for most analyses. Analyses with high Si contents (>0.20 wt% SiO_2) were discarded for being contaminated by the silicate matrix.

IR SPECTROSCOPY

An infrared spectrum (Fig. 2) of powdered argandite was recorded in the range 4000 and 650 cm^{-1} using a Nicolet 5700 FTIR spectrometer equipped with a Nicolet Continuum IR microscope and a diamond-anvil cell. Bands at 3550 , 3485 , and 3340 cm^{-1} belong to the stretching vibrations of the hydroxyl groups. Based on the empirical correlation established by Libowitzky (1999), the values of the ν_{OH} vibrational frequencies indicate the presence of weak hydrogen bonds in the structure of argandite, with O...O distances of ~ 2.76 – 3.00 Å, which compares to the observed distances of 2.916 – 3.122 Å. A band at 984 cm^{-1} , with a shoulder at 1022 cm^{-1} , can be assigned to the ν_3 vibration of VO_4 tetrahedra and a band at 728 cm^{-1} to the ν_1 vibration of VO_4 tetrahedra. Note that the bands due to the vibrations of the VO_4 tetrahedra are overlapped by bands due to the AsO_4 vibrations as a result of the AsO_4^{3-} for VO_4^{3-} substitution.

POWDER X-RAY DIFFRACTION STUDY

The X-ray powder diffraction pattern of argandite was collected using a 114.6 mm diameter Gandolfi camera and $CuK\alpha_1$ /

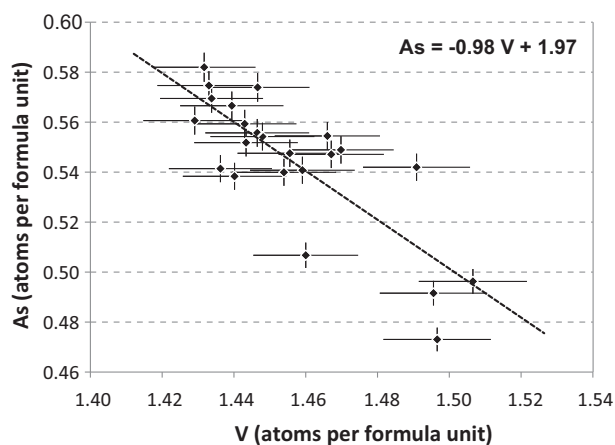


FIGURE 1. Arsenic vs. vanadium correlation in argandite. Errors are estimated 1σ from the electron microprobe analyses (1%).

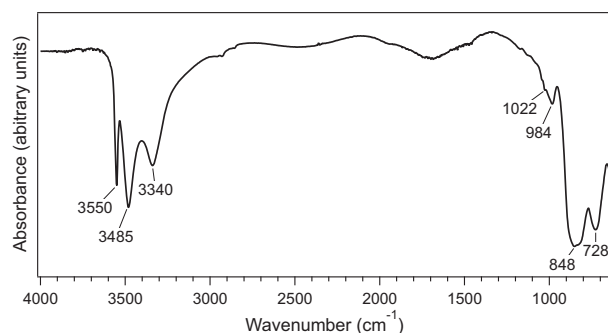


FIGURE 2. FTIR spectrum of powdered argandite. The depression at ~ 1680 cm^{-1} is attributed to adsorbed water.

Ni-filtered X-ray radiation ($\lambda = 1.540593$ Å). The powder pattern is in good agreement with the results of the crystal-structure analysis in terms of the comparison between calculated and observed d -spacings and intensities (Table 2). The unit-cell parameters were refined using the least-squares method as implemented in the program UnitCell (Holland and Redfern 1997) and converged to: $a = 5.530(1)$, $b = 12.253(1)$, $c = 10.116(1)$ Å, $\beta = 95.87(2)^\circ$, $V = 681.85(14)$ Å³, in good agreement with those obtained by single-crystal diffraction (Table 3).

TABLE 2. X-ray powder diffraction data for argandite

l_{obs}	d_{obs}	l_{calc}	d_{calc}	h	k	l
		52	7.769	0	1	1
10	5.053	{ 9	5.021	0	0	2
		{ 16	5.016	1	0	1
		{ 19	4.643	1	1	1
30	4.095	18	4.083	1	2	0
		7	3.785	0	3	1
50	3.708	{ 33	3.711	1	1	2
		{ 17	3.690	1	2	1
60	3.395	14	3.394	1	1	2
30	3.302	47	3.287	1	2	2
30	3.226	59	3.229	0	1	3
		6	3.170	0	3	2
100	3.074	{ 100	3.061	1	3	1
		{ 5	3.061	1	2	2
50	2.945	{ 36	2.932	0	4	1
		{ 12	2.903	1	1	3
30	2.751	31	2.739	1	0	3
		9	2.686	1	2	3
70	2.687	{ 24	2.674	1	4	0
		{ 22	2.673	1	1	3
		11	2.645	2	1	1
		8	2.616	0	4	2
		10	2.590	0	3	3
50	2.522	{ 8	2.522	2	1	1
		{ 11	2.511	0	0	4
		{ 77	2.508	2	0	2
		9	2.499	2	2	0
		10	2.477	2	2	1
		15	2.412	1	3	3
40	2.324	15	2.376	2	2	1
		39	2.315	1	4	2
		11	2.275	1	3	3
		10	2.261	0	4	3
		14	2.192	2	1	3
		9	2.166	1	5	1
		10	2.051	1	3	4
		12	1.997	2	1	3
		24	1.947	2	0	4
		9	1.923	2	1	4
		11	1.892	1	6	1
		16	1.876	1	4	4
40	1.791	39	1.788	1	4	4
		18	1.766	2	0	4
		8	1.758	1	3	5
		16	1.725	0	7	1
		6	1.697	1	2	4
		12	1.684	2	1	5
30	1.677	{ 13	1.674	0	0	6
		{ 10	1.669	1	3	5
		{ 20	1.668	3	3	1
		7	1.657	3	1	3
		8	1.649	2	5	3
		9	1.638	1	5	4
20	1.594	8	1.584	2	6	2
30	1.572	39	1.568	3	4	0
		13	1.552	0	7	3
30	1.530	{ 27	1.533	0	8	0
		{ 14	1.531	2	6	2
		{ 18	1.450	1	4	6

Note: l_{calc} calculated with program LAZY PULVERIX (Yvon et al. 1977); only reflections with $l_{calc} \geq 5$ are listed.

TABLE 3. Comparison of unit-cell parameters obtained by different methods for argandite from Pipji (room-temperature measurements)

	Single crystal Australian Synchrotron $\lambda = 0.773418 \text{ \AA}$	Single crystal Xcalibur E $\lambda = 0.71073 \text{ \AA}$	Powder pattern Gandolfi camera $\lambda = 1.540593 \text{ \AA}$
<i>a</i> (Å)	5.498(11)	5.5038(2)	5.530(1)
<i>b</i> (Å)	12.265(3)	12.2665(5)	12.253(1)
<i>c</i> (Å)	10.092(2)	10.1055(5)	10.116(1)
β (°)	95.594(3)	95.559(4)	95.87(2)
<i>V</i> (Å ³)	677.3(2)	679.04(5)	681.85(14)

SINGLE-CRYSTAL X-RAY DIFFRACTION STUDY

Experimental methods

Single-crystal intensity data were originally collected at the Australian Synchrotron PX1 beamline, using a crystal of about $30 \times 25 \times 25 \mu\text{m}^3$. Intensity data were collected using a ADSC Quantum 210r detector using monochromatic X-radiation ($\lambda = 0.773418 \text{ \AA}$) by scanning in ϕ and ω with frame widths of 2° and 10 s counting time per frame. The unit-cell dimensions, refined using least-squares techniques, are $a = 5.498(11)$, $b = 12.265(3)$, $c = 10.092(2) \text{ \AA}$, $\beta = 95.594(3)^\circ$, and $V = 677.3(2) \text{ \AA}^3$ (Table 3). The crystal structure was solved using direct methods and refined to $R1(F) = 6.52\%$ and $wR2(F^2) = 18.57\%$ for 992 observed reflections with $F_o > 4\sigma(F_o)$. The refined crystal structure is similar to that presented below; however, negative displacement parameters for the O positions prevent us to present the full data here. Unusually small atomic displacement parameters for small molecules measured at the PX1 beamline result from incomplete absorption in the CCD phosphor of high-energy photons, which leads to a variation in the measured signal depending on the path-length of the diffracted photon through the phosphor (Hester and Edward 2010, written communication).

Consequently, we succeeded in extracting a larger crystal ($58 \times 48 \times 42 \mu\text{m}^3$), which was measured on an Oxford Diffraction Xcalibur E diffractometer using MoK α X-ray radiation. Details of the data collection are reported in Table 4. The data were processed using the CrysAlisPro program (Oxford Diffraction 2009) and corrected for Lorentz and polarization effects. An empirical absorption correction was applied using the SCALE3 ABSPACK algorithm, as implemented in CrysAlisPro. The unit-cell dimensions [$a = 5.5038(2)$, $b = 12.2665(5)$, $c = 10.1055(5) \text{ \AA}$, $\beta = 95.559(4)^\circ$, $V = 679.04(5) \text{ \AA}^3$] are within error of the dimensions measured on the crystal measured at the PX1 beamline, except for a $\sim 0.1\%$ extension of the *c*-axis and a slight decrease in the β -angle (Table 3). The crystal structure was solved in space group $P2_1/n$ by direct methods using SHELXS-97 and refined by full-matrix least-squares on F^2 , using SHELXL-97 (Sheldrick 2007). (CIF¹ is available on deposit.) The H atom positions were deduced from the difference-Fourier syntheses and H–O distances were constrained to be 0.98 \AA from the associated O atoms. The final *R1* index with anisotropic displacement parameters for all but the H positions was 3.40% for 1661 observed reflections with $F_o > 4\sigma(F_o)$ and 133 refined parameters ($wR2 = 5.04\%$).

¹ Deposit item AM-11-061, CIF. Deposit items are available two ways: For a paper copy contact the Business Office of the Mineralogical Society of America (see inside front cover of recent issue) for price information. For an electronic copy visit the MSA web site at <http://www.minsocam.org>, go to the American Mineralogist Contents, find the table of contents for the specific volume/issue wanted, and then click on the deposit link there.

Crystal structure and relations with other minerals

Fractional atomic coordinates, isotropic displacement parameters, and site occupancy factors for argandite are listed in Table 5; selected interatomic distances are shown in Table 6; bond-valence calculations in Table 7; and details of the hydrogen bonding in argandite are listed in Table 8. The crystal structure of argandite contains four Mn sites, each coordinated by six O atoms, and one V site coordinated by four O atoms. Four out of the eight oxygen positions correspond to hydroxyl groups coordinated to Mn sites. Occupancy refinement of the V site led values similar to the measured As contents ($V_{1.46}As_{0.54}$; Tables 1 and 5). Refinement of the occupancy of the Mn sites showed that Mn1 and Mn2 are fully occupied, while occupancy factors of 0.92 and 0.94 were obtained for the Mn3 and Mn4 sites, respectively, consistent with the incorporation of minor Mg revealed by the chemical analysis (Table 1) on these sites. Bond-valence calculations confirm that Mn is present in the divalent state (bond-valence sums 1.92–2.11). The bond-valence sums also confirm the hydrogen positions obtained from the crystal structure refinement (Table 7). The crystal structure consists of alternating octahedral (O) and octahedral-tetrahedral (OT) layers (Fig. 3). Within the O layers, edge-sharing $Mn3O_2(OH)_4$ and $Mn4O_2(OH)_4$ octahedra form strips that extend along [100]. The strips link in the **b** direction via corner-sharing $Mn1O_4(OH)_2$ octahedra to form a sheet parallel to (001) (Fig. 4). Corner-sharing $Mn2O_2(OH)_4$ octahedra and VO_4 tetrahedra form chains that extend along [010]. The O and OT layers link into a heteropolyhedral framework with each $Mn2O_2(OH)_4$ octahedron sharing a face with a $Mn4O_2(OH)_4$ octahedron, an edge with a $Mn1O_4(OH)_2$ octahedron, and also linking to an O6

TABLE 4. Crystal data, data collection, and refinement details for argandite

Crystal data	
Space group	$P2_1/n$
<i>a, b, c</i> (Å)	5.5038(2), 12.2665(5), 10.1055(5)
β (°)	95.559(4)
<i>V</i> (Å ³), <i>Z</i>	679.04(5), 2
<i>F</i> (000)	725
μ (mm ⁻¹)	8.635
Crystal dimensions (mm)	0.058 × 0.048 × 0.042
Data collection	
Diffractometer	Oxford Diffraction Xcalibur E
Temperature (K)	123
Wavelength	MoK α , $\lambda = 0.71073 \text{ \AA}$
θ range (°)	2.62–29.14
Detector distance (mm)	45.44
Rotation axes	ω
Rotation width (°)	1.0
Total no. of frames	518
Collection time per frame (s)	20
<i>h, k, l</i> ranges	–7 → 6, –16 → 15, –13 → 13
Total reflections measured	7752
Data completeness (%)	90.2
Unique reflections	1661 ($R_{int} = 0.0614$)
Refinement	
Refinement on	F^2
$R1^*$ for $F_o > 4\sigma(F_o)$	3.40%
$wR2^\dagger$ for all F_o^2	5.04%
Reflections used $F_o > 4\sigma(F_o)$	1661
Number of parameters refined	133
Extinction factor	0.0010(2)
$\Delta\rho_{min}, \Delta\rho_{max}$ (e/Å ³)	0.775, –0.743
Goof	1.020

* $R1 = \sum ||F_o| - |F_c|| / \sum |F_o|$.

† $wR2 = \sum w(|F_o|^2 - |F_c|^2)^2 / \sum w|F_o|^2$; $w = 1/[\sigma^2(F_o^2) + (0.042P)^2 + 12.60P]$; $P = [(max(0 \text{ or } F_o^2)) + 2F_c^2]/3$.

TABLE 5. Fractional atomic coordinates, isotropic displacement parameters (in \AA^2), and site occupancy factors for argandite

Atom	x	y	z	U_{eq}	U_{11}	U_{22}	U_{33}	U_{12}	U_{13}	U_{23}
V*	0.53430(10)	0.42008(4)	0.70834(6)	0.0079(2)	0.0074(3)	0.0082(3)	0.0078(4)	0.0004(3)	-0.0002(2)	-0.0001(2)
Mn1	0	0.5	0.5	0.0105(3)	0.0117(5)	0.0098(5)	0.0098(6)	-0.0010(4)	0.0003(4)	-0.0016(4)
Mn2	0.23235(11)	0.17921(5)	0.79338(7)	0.0120(2)	0.0112(4)	0.0119(4)	0.0124(4)	0.0019(3)	-0.0019(3)	-0.0008(3)
Mn3†	0.74927(11)	0.56820(5)	0.99173(7)	0.0095(2)	0.0072(4)	0.0094(4)	0.0116(4)	-0.0002(3)	-0.0003(3)	0.0001(3)
Mn4‡	0.24910(11)	0.20769(5)	0.50088(7)	0.0103(2)	0.0100(4)	0.0104(4)	0.0105(4)	-0.0012(3)	0.0006(3)	0.0000(3)
OH1	0.0535(5)	0.3060(2)	0.8875(3)	0.0138(7)	0.0139(15)	0.0149(16)	0.0126(17)	0.0008(13)	0.0008(13)	-0.0005(12)
O2	0.5617(4)	0.42947(19)	0.8817(3)	0.0126(7)	0.0104(15)	0.0143(15)	0.0126(16)	0.0004(13)	-0.0014(12)	-0.0002(11)
OH3	0.0784(5)	0.3449(2)	0.4060(3)	0.0156(7)	0.0128(16)	0.0156(15)	0.0183(19)	-0.0007(14)	0.0009(13)	0.0005(12)
O4	0.4159(5)	0.2965(2)	0.6677(3)	0.0177(8)	0.0232(17)	0.0135(16)	0.0156(18)	-0.0016(13)	-0.0021(14)	-0.0046(12)
OH5	0.0749(5)	0.5612(2)	0.8870(3)	0.0152(7)	0.0123(15)	0.0138(16)	0.0192(18)	-0.0011(13)	0.0008(13)	0.0004(11)
OH6	0.5433(5)	0.6824(2)	0.8724(3)	0.0151(7)	0.0139(16)	0.0157(16)	0.0158(17)	0.0028(14)	0.0018(13)	-0.0017(12)
O7	0.3496(5)	0.5203(2)	0.6375(3)	0.0154(7)	0.0162(16)	0.0127(15)	0.0165(18)	0.0026(13)	-0.0025(13)	0.0029(12)
O8	0.8205(5)	0.4273(2)	0.6616(3)	0.0182(7)	0.0135(16)	0.0270(17)	0.0142(17)	0.0048(14)	0.0016(13)	0.0017(12)
H1	0.013(8)	0.347(3)	0.807(3)	0.053§						
H3	0.193(6)	0.361(4)	0.342(4)	0.053§						
H5	0.056(8)	0.527(3)	0.801(3)	0.053§						
H6	0.640(7)	0.746(2)	0.864(5)	0.053§						

* Refined occupancy $V_{1.46(2)As_{0.54(2)}}$.† Refined occupancy $Mn_{0.92(2)}$.‡ Refined occupancy $Mn_{0.94}$.§ U_{eq} for hydrogen atoms were constrained to be equal to each other during refinement.**TABLE 6.** Selected interatomic distances (\AA) for argandite

Mn1	O8	2.180(3)	Mn3	OH6	2.107(3)
	O8	2.180(3)		OH5	2.170(3)
	OH3	2.187(3)		OH5	2.175(3)
	OH3	2.187(3)		OH1	2.189(3)
	O7	2.275(2)		O2	2.231(2)
	O7	2.275(2)		O2	2.234(3)
<Mn1-O>		2.214	<Mn3-O>		2.184
Mn2	OH1	2.115(3)	Mn4	OH3	2.112(3)
	O7	2.133(2)		OH1	2.126(3)
	OH3	2.143(3)		O4	2.138(3)
	OH6	2.149(3)		OH6	2.173(3)
	O4	2.225(3)		O2	2.259(2)
	OH5	2.628(3)		OH5	2.289(2)
<Mn2-O>		2.232	<Mn4-O>		2.183
V	O4	1.685(2)			
	O8	1.690(3)			
	O7	1.708(2)			
	O2	1.747(3)			
<V-O>		1.707			

TABLE 7. Bond-valence analysis for argandite

	Mn1	Mn2	Mn3	Mn4	V	H1	H3	H5	H6	Sum excl.H	Sum incl.H
OH1	0.42	0.34	0.40			0.87				1.16	2.03
O2			0.30	0.28	1.14					2.02	2.02
			0.30								
OH3	0.34	0.39		0.42			1.00			1.15	2.15
	0.34										
O4		0.31		0.39	1.32					2.02	2.02
OH5		0.10	0.36	0.26				0.91		1.07	1.98
			0.35								
OH6		0.38	0.42	0.36					0.92	1.16	2.08
O7	0.27	0.40			1.26					1.93	1.93
	0.27										
O8	0.35			1.34	0.13			0.09	0.08	1.69	1.99
	0.35										
	1.92	2.00	2.07	2.11	5.06	1.00	1.00	1.00	1.00		

Note: Calculations made using the program VALENCE (Brown 1996) and the parameters of Brown and Altermatt (1985).

anion that coordinates to Mn3 and Mn4 (Fig. 3). The four oxygen atoms of the VO_4 tetrahedron also belong to $Mn\phi_6$ octahedra ($\phi = O, OH$) from the O-sheets, with O2 coordinating to two Mn3 and one Mn4 cations, O7 to Mn1, O4 to Mn4, and O8 to Mn1.

TABLE 8. Details of hydrogen bonding in argandite (angstroms, degrees), and comparison with allactite (Moore 1968) and raadeite (Chopin et al. 2001)

$D-H\cdots A$	D-H	H $\cdots A$	$D\cdots A$	$\angle D-H\cdots A$	$D\cdots A$	$D\cdots A$
					Allactite	Raadeite
OH1-H1 \cdots O8 ⁱ	0.965(19)	1.99(2)	2.916(4)	161(4)	2.878	2.895
OH5-H5 \cdots O8 ⁱⁱ	0.961(19)	2.19(3)	3.038(4)	146(4)	3.020	2.946
OH6-H6 \cdots O8 ⁱⁱⁱ	0.951(19)	2.25(3)	3.122(4)	151(4)	3.058	3.055

Symmetry codes for argandite: (i) x, y, z - 1; (ii) x, y, z; (iii) -x + 1/2, y + 1/2, -z + 3/2.

Within the OT layer, the O4 and O7 anions link the VO_4 group and the $Mn_2O_2(OH)_4$ octahedra into chains. The bond-valence sums (Table 7) indicate that, without the contribution of hydrogen bonds, the O8 anion is substantially underbonded. The O8 anion thus acts as a hydrogen-bond acceptor for hydrogen bonds emanating from OH1, OH5, and OH6 (Table 8). These weak hydrogen bonds provide the necessary increase in bond valence, and contribute to the strengthening of the framework.

Argandite is the V analog of allactite, $Mn_7(AsO_4)_2(OH)_8$ (Moore 1968), and is also isostructural with raadeite, $Mg_7(PO_4)_2(OH)_8$ (Chopin et al. 2001). The unit-cell volume of argandite is 0.7% larger than that of allactite (Table 9); this is consistent with the larger size the tetrahedral site in argandite compared to allactite: the average V-O distance in argandite is 1.6% longer than the As-O distance in allactite. Moore (1968) did not discuss the hydrogen bonding for allactite. Chopin et al. (2001) suggested a H-bonding scheme for raadeite similar to that described above for argandite; they did however propose an additional H bond (OH3-H3 \cdots O8) along a polyhedral edge; it is unlikely that an H bond will form along the edge of a coordination polyhedron, except where the coordination polyhedron involves a monovalent cation of high coordination number (Baur 1972, 1973). Based on the distance between the oxygen atom from the hydroxyl group and the donor oxygen atom, the hydrogen bonding is weakest in argandite and strongest in raadeite (Table 8).

The formula and unit-cell parameters of argandite also show some relations with waterhouseite, $Mn_7(PO_4)_2(OH)_8$ (Pring et al. 2005) (Table 9). Unlike argandite, the crystal structure of waterhouseite does not contain face-sharing MnO_6 octahedra, and the XO_4 tetrahedra ($X = V, As$ in allactite-type structures,

TABLE 9. Comparison of argandite with related species

	Argandite	Allactite	Raadeite	Waterhouseite
Reference	This work	Moore (1968)	Chopin et al. (2001)	Pring et al. (2005)
Formula	$Mn_7(VO_4)_2(OH)_8$	$Mn_7(AsO_4)_2(OH)_8$	$Mg_7(PO_4)_2(OH)_8$	$Mn_7(PO_4)_2(OH)_8$
Symmetry	monoclinic	monoclinic	monoclinic	monoclinic
Space group	$P2_1/n$	$P2_1/n$	$P2_1/n$	$P2_1/c$
<i>a</i> (Å)	5.5038(2)	5.51*	5.250(1)	11.364(6)
<i>b</i> (Å)	12.2665(5)	12.12*	11.645(2)	5.570(2)
<i>c</i> (Å)	10.1055(5)	10.12*	9.655(2)	10.455(3)
β (°)	95.559(4)	95.73*	95.94(1)	96.61(3)
<i>V</i> (Å ³)	679.04(5)	672.4	587.2	657.4(2)
<i>Z</i>	2	2	2	2
Strongest lines in the X-ray powder pattern	3.708 (50), 3.395 (60), 3.074 (100), 2.945 (50), 2.687 (70)	3.043 (100), 3.720 (54), 3.284 (48), 3.235 (44), 2.902 (39)	7.46 (60), 4.748 (60), 4.436 (75), 3.598 (60), 3.521 (80), 3.145 (70), 3.087 (70), 2.905 (100), 2.794 (75), 2.199 (80)	4.436 (70), 3.621 (100), 3.069 (50), 2.941 (40), 2.780 (35)
<i>D</i> _{meas} ; <i>D</i> _{calc}	3.71; 3.68	3.83; 3.94	n.d.; 2.806	3.591
Mohs hardness	~3.5–4	4.5	n.d.	~4
α	~1.74	1.755	1.5945(5)	1.730(3)
β	1.762(4)	1.772	1.6069(5)	~1.738
γ	~1.77	1.774	1.6088(5)	1.738(4)
Opt. character	biaxial negative	biaxial negative	biaxial negative	biaxial negative
2 <i>V</i> (meas); (calc)	n.d.; ~62°	75–82°; n.d.	70.5–76°; 75–75.6°	n.d.
Megascopic color	Orange	Greenish, reddish, pink, brownish gray	Colorless	Orange-brown to dark clove-brown
Habit	Rounded, anhedral grains	Prismatic, elongated on [010], bladed and tabular on {100}, divergent or subparallel aggregates	Nodules composed of rounded tabular plates, flattened on [010], botryoidal crusts	Divergent sprays of bladed crystals, elongated parallel to [001]
Twinning	none observed	none	none	// to (100)

* Reduced cell. The cell given by Moore (1968) is non-reduced: $a = 11.03 \text{ \AA}$, $b = 12.12 \text{ \AA}$, $c = 5.51 \text{ \AA}$, $\beta = 114.1^\circ$, space group $P2_1/a$.

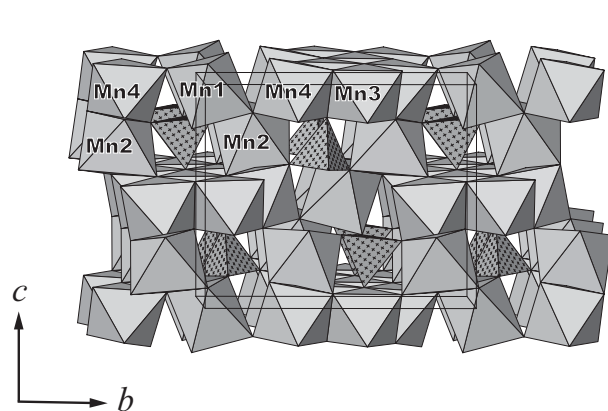


FIGURE 3. The crystal structure of argandite viewed along a direction close to [100]. $Mn(O,OH)_6$ octahedra are labeled with the site names (Table 5), and VO_4 tetrahedra are highlighted with crosses. The unit cell is outlined. All structure drawings were completed using ATOMS (Shape Software 1997).

and P in waterhouseite) in waterhouseite are linked to the MnO_6 octahedra not only via their corners, but also via their edges.

Chemically, argandite is the fourth known Mn vanadate, after reppiaite, $Mn_3(VO_4)_2(OH)_4$ (Basso et al. 1992), fianelite, $Mn_2V(V,As)O_7 \cdot 2H_2O$ (Brugger and Berlepsch 1996), and ansermetite, $MnV_2O_6 \cdot 4H_2O$ (Brugger et al. 2003). Remarkably, the occurrence of the four minerals has so far been restricted to metamorphosed sediment-hosted exhalative (or near-seafloor) Mn-deposits of the Central Alps (e.g., Brugger and Gieré 2000; Brugger and Meisser 2006; Cortesogno et al. 1979).

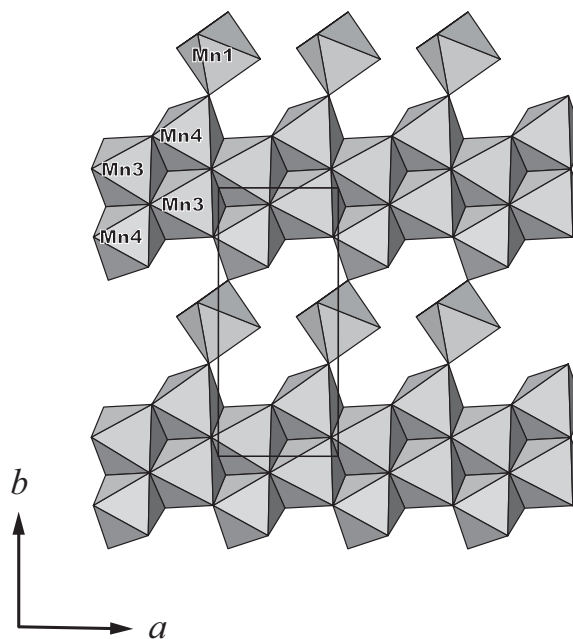


FIGURE 4. Octahedral layers in the crystal structure of argandite viewed along [001]. The unit cell is outlined.

ACKNOWLEDGMENTS

We are grateful to John Terlet, Peter Self, and Linda Matto (Adelaide Microscopy) for help with the EMP measurements, to Pascal Tschudin and Peter O. Baumgartner (SEM/EDXS laboratory, Institute of Geology and Paleontology, UNIL, Lausanne) for the help with the SEM. Special thanks to Philippe Thélin (XRD laboratory, Institute of Mineralogy and Geochemistry, UNIL, Lausanne) for

providing XRD-powder microanalysis facilities. Hayley Brown provided assistance with collection of the infrared spectrum. Part of this research was undertaken on the PX1 beamline at the Australian Synchrotron, Victoria, Australia; thanks to Tom Caradoc-Davies for his help at the beamline. The paper benefitted from careful reviews by Uwe Kolitsch and Michael Schindler.

REFERENCES CITED

- Argand, É. (1911) Les nappes de recouvrement des Alpes pennines et leurs prolongements structuraux. *Matériaux pour la Carte Géologique de la Suisse*, 31, 1–26.
- (1916) Sur l'arc des Alpes Occidentales. *Eclogae Geologicae Helveticae*, 14, 145–204.
- Basso, R., Lucchetti, G., Zefiro, L., and Palenzona, A. (1992) Reppiaite, $Mn_3(OH)_4(VO_4)_2$, a new mineral from Val Graveglia (Northern Apennines, Italy). *Zeitschrift für Kristallographie*, 201, 223–234.
- Baur, W.H. (1972) Prediction of hydrogen bonds and hydrogen atom positions in crystalline solids. *Acta Crystallographica*, B28, 1456–1465.
- (1973) Criteria for hydrogen bonding. II. A hydrogen bond in the edge of a coordination polyhedron around a cation. *Acta Crystallographica*, B29, 139–140.
- Bowell, R.J. (1994) Sorption of arsenic by iron oxides and oxyhydroxides in soils. *Applied Geochemistry*, 9, 279–286.
- Brown, I.D. (1996) VALENCE: a program for calculating bond valences. *Journal of Applied Crystallography*, 29, 479–480.
- Brown, I.D. and Altermatt, D. (1985) Bond-valence parameters obtained from a systematic analysis of the inorganic crystal structure database. *Acta Crystallographica*, B41, 244–247.
- Brugger, J. and Berlepsch, P. (1996) Description and crystal structure of fianelite $Mn_2(V,As)O_7 \cdot 2H_2O$, a new mineral from Fianel, Val Ferrera, Graubünden, Switzerland. *American Mineralogist*, 81, 1270–1276.
- (1997) Johnnesite $Na_2(Mn^{2+})_6(Mg,Mn)_7(AsO_4)_2(Si_6O_{17})_2(OH)_8$: a new occurrence in the Val Ferrera (Graubünden, Switzerland). *Schweizerische Mineralogische und Petrographische Mitteilungen*, 77, 449–455.
- Brugger, J. and Gieré, R. (1999) As, Sb, and Ce enrichment in minerals from a metamorphosed Fe-Mn deposit (Val Ferrera, Eastern Swiss Alps). *Canadian Mineralogist*, 37, 37–52.
- (2000) Origin and distribution of some trace elements in metamorphosed Fe-Mn deposits, Val Ferrera, Eastern Swiss Alps. *Canadian Mineralogist*, 38, 1075–1101.
- Brugger, J. and Meisser, N. (2006) Manganese-rich assemblages in the Barrhorn Unit, Turtmannal, Central Alps, Switzerland. *Canadian Mineralogist*, 44, 229–248.
- Brugger, J., Gieré, R., Graeser, S., and Meisser, N. (1997) The crystal chemistry of roméite. *Contributions to Mineralogy and Petrology*, 127, 136–146.
- Brugger, J., Gieré, R., Grobety, B., and Uspensky, E. (1998) Scheelite-powellite and paraniite-(Y) from Fianel, Val Ferrera, GR (Swiss Alps). *American Mineralogist*, 83, 1100–1110.
- Brugger, J., Armbruster, T., Meisser, N., Hejny, C., and Grobety, B. (2001) Description and crystal structure of turtmannite, a new mineral with a 68 Å period related to megovermite. *American Mineralogist*, 86, 1494–1505.
- Brugger, J., Berlepsch, P., Meisser, N., and Armbruster, T. (2003) Ansermetite, $MnV_2O_6 \cdot 4H_2O$, a new mineral species with V^{5+} in five-fold coordination from Val Ferrera, Eastern Swiss Alps. *Canadian Mineralogist*, 41, 1423–1431.
- Brugger, J., Krivovichev, S., Meisser, N., Ansermet, S., and Armbruster, T. (2006) Scheuchzerite, $Na(Mn,Mg)_3[VSi_6O_{28}(OH)](OH)_3$, a new single-chain silicate. *American Mineralogist*, 91, 937–943.
- Chopin, C., Ferraris, G., Prencipe, M., Brunet, F., and Medenbach, O. (2001) Raadeite, $Mg_7(PO_4)_2(OH)_8$: a new dense-packed phosphate, from Modum (Norway). *European Journal of Mineralogy*, 13, 319–327.
- Cortesogno, L., Lucchetti, G., and Penco, A.M. (1979) Le mineralizzazioni a manganese nei diaspri delle ofioliti liguri: mineralogia e genesi. *Rendiconti della Società Italiana di Mineralogia e Petrologia*, 35, 151–197.
- Escher, A., Masson, H., and Steck, A. (1987) Coupes géologiques des Alpes occidentales suisses. Service Hydrologique et Géologique National, Rapports Géologiques No. 2, 11 pp. (with tables).
- Gerlach, H. (1869) Die Penninischen Alpen. *Denkschrift Schweizer Naturforschendes Gesellschaft*, 23, 1–68.
- Holland, T.J.B. and Redfern, S.A.T. (1997) Unit cell refinement from powder diffraction data: the use of regression diagnostics. *Mineralogical Magazine*, 61, 65–77.
- Libowitzky, E. (1999) Correlation of O-H stretching frequencies and O-H...O hydrogen bond lengths in minerals. *Monatshefte für Chemie*, 130, 1047–1059.
- Mandarino, J.A. (1976) The Gladstone-Dale relationship. Part I: derivation of new constants. *Canadian Mineralogist*, 14, 498–502.
- (2007) The Gladstone-Dale compatibility of minerals and its use in selecting mineral species for further study. *Canadian Mineralogist*, 45, 1307–1324.
- Moore, P.B. (1968) Crystal chemistry of the basic manganese arsenate minerals: II. The crystal structure of allactite. *American Mineralogist*, 53, 733–741.
- Oxford Diffraction (2009) CrysAlisPro. Oxford Diffraction, Yarnton, England.
- Pring, A. (1995) The place of descriptive mineralogy in modern science. *The Australian Mineralogist*, 1, 3–7.
- Pring, A., Kolitsch, U., and Birch, W.D. (2005) Description and unique crystal structure of waterhouseite, a new hydroxy manganese phosphate from the Iron Monarch deposit, Middleback Ranges, South Australia. *Canadian Mineralogist*, 43, 1401–1410.
- Sartori, M. (1990) L'unité du Barrhorn. *Mémoire de Géologie (Lausanne)*, 6, 156 p.
- Shape Software (1997) ATOMS for Windows and Macintosh V 4.0, Kingsport, Tennessee, U.S.A.
- Sheldrick, G.M. (2007) A short history of SHELX. *Acta Crystallographica*, A64, 112–122.
- Sherman, D.M. and Randall, S.R. (2003) Surface complexation of arsenic(V) to iron(III) (hydr)oxides: Structural mechanism from ab initio molecular geometries and EXAFS spectroscopy. *Geochimica et Cosmochimica Acta*, 67, 4223–4230.
- Yvon, K., Jeitschko, W., and Parthé, E. (1977) LAZY PULVERIX, a computer program, for calculating X-ray and neutron diffraction powder patterns. *Journal of Applied Crystallography*, 10, 73–74.

MANUSCRIPT RECEIVED MARCH 25, 2011

MANUSCRIPT ACCEPTED JULY 31, 2011

MANUSCRIPT HANDLED BY ANDREW McDONALD